Proseminarium Fotoniki

Proseminarium Fotoniki 1103-4Fot25, pon 15.15-16.45, Pasteura 5, s. **B4.61**

Rafał Kotyński, Piotr Wróbel

Daty spotkań:
2018-02-26 – wstęp
2018-03-05 – wybór tematów
12, 19, 26 marca
9, 16, 23,30 kwietnia
7,14,21,28 maja
4, 11 czerwca

Aleksandra Adamczyk
Karolina Łempicka
Bartłomiej Sowiński
Weronika Zielony

Zasada zaliczenia:
- każdy student przygotowuje i wygłasza w semestrze po 2 seminaria na uzgodniony temat dotyczący optyki współczesnej
- jedno z seminariów należy wygłosić w jęz. angielskim
- na każde seminarium przeznaczonych będzie 45min oraz 10min na dyskusję po jego zakończeniu

- tematem przewodnim proseminarium w tym roku będzie teoria oszczędnego próbkowania (ang. Compressive Sensing/Sampling)

Propozycje tematów

Oszczędne próbkowanie (CS - Compressive sensing/sampling)

- **Szybka detekcja jednopunktowa**
- **Wykorzystanie CS do “widzenia zza rogu”**
- **Wykorzystanie CS do obrazowania przez ośrodki rozpraszające**
- **Wykorzystanie CS w holografii**
- **Matematyczne podstawy oszczędnego próbkowania**
- Obrazowanie pośrednie, kamery jednopunktowe (comptational ghost imaging, single-pixel dectectors)
- Wykorzystanie CS do pomiaru odległości, radar laserowy (ladar)
- Wykorzystanie CS do rekonstrukcji obrazu na podstawie zbioru skanów – zastosowanie w mikroskopii skaningowej i rezonansie magnetycznym (MRI)
- Wykorszystanie CS do uzyskania obrazowania nadrozdzielczego
- Właściwości i wykorzystanie transformat liniowych: a) Hadamarda, Fouriera, DCT; b) falkowe, szumkowe (ang. noislets)
- Podstawy programowania liniowego – wykorazystanie do rekonstrukcji pomiaru
- Przegląd narzędzi numerycznych do obliczeń CS (do rekonstrukcji sygnału)

Propozycje tematów

Inne tematy

- Własne propozycje, np. temat pracy licencjackiej / magisterskiej
- Opis wybranej metody modelowania elektromagnetycznego wraz z jej (najlepiej wolnodostępną) implementacją
- Cloaking
- Slow light
- Siatki podfalowe – metalowe, lub o wysokim kontraście
- Absorbery elektromagnetyczne

Motywacja:

The goal of image compression is to represent the digital model of an object as compactly as possible. ***One can regard the the possibility of digital compression as a failure of sensor design. If it is possible to compress measured data, one might argue that too many measurements were taken****.*

David Brady

Oszczędne próbkowanie:

Jeśli nie zależy nam na redundancji w pomiarze i jeśli mierzony sygnał jest kompresowalny (istnieje dla sygnału reprezentacja rzadka), można myśleć o uproszczeniu układu pomiarowego i zmniejszeniu liczby mierzonych danych.
W optyce, takie postępowanie pozwala często bardzo uprościć układ detektora/kamery. Sygnał wymaga następnie rekonstrukcji cyfrowej.

Computational ghost imaging

(Pomiar pośredni, koincydencyjny)

J. H. Shapiro, Computational ghost imaging, Phys. Rev. A 78, 061802(R),2008

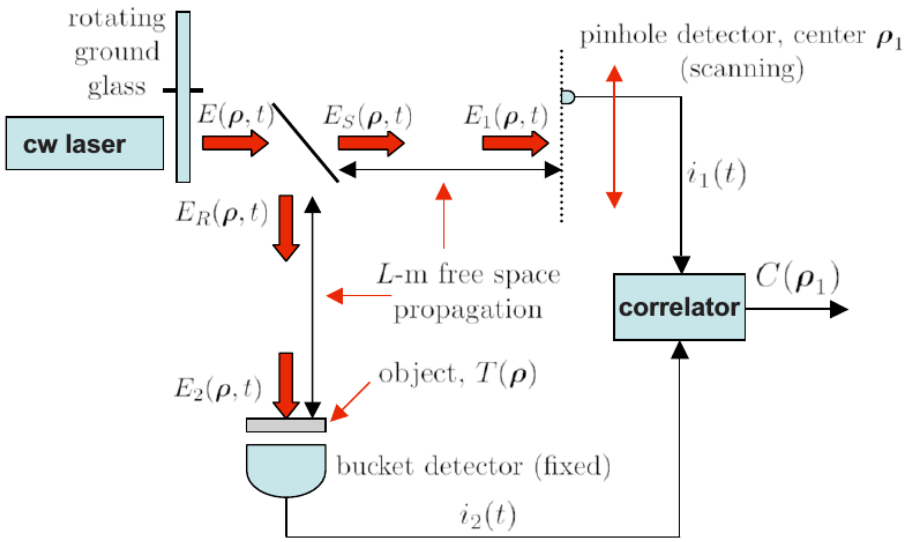

FIG. 1. (Color online) Pseudothermal ghost-imaging setup.

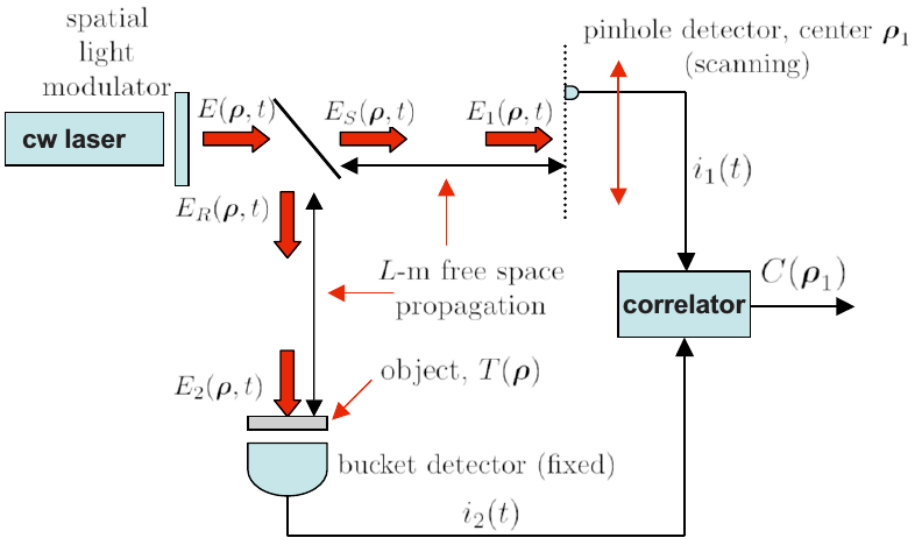

FIG. 2. (Color online) SLM ghost-imaging setup.

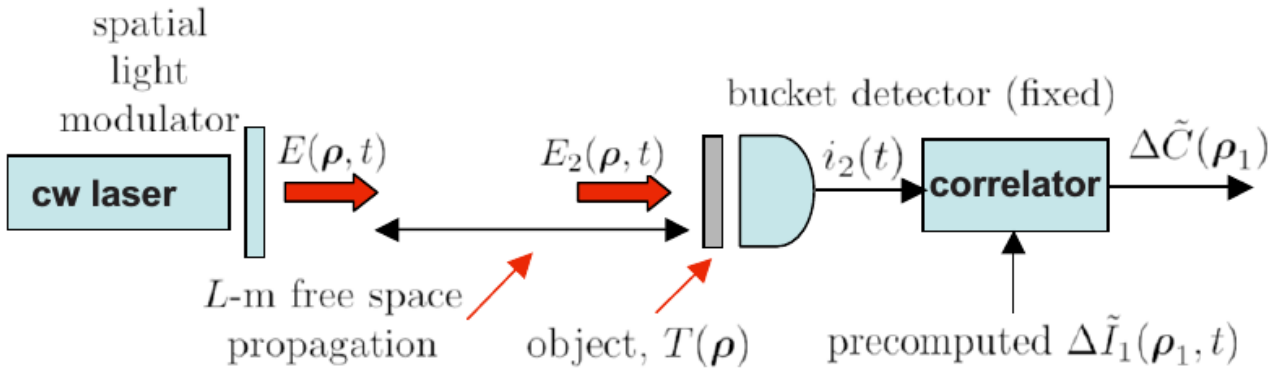

FIG. 3. (Color online) Computational ghost-imaging setup.

Computational ghost imaging

Y. Bromberg et al, Ghost imaging with a single detector, Phys. Rev A 79, 053840, 2009

We experimentally demonstrate pseudothermal ghost imaging and ghost diffraction using only a single detector. We achieve this by replacing the high-resolution detector of the reference beam with a computation of the propagating field, following a recent proposal by Shapiro, Phys. Rev. A 78, 061802(R) (2008). Since only a single detector is used, this provides experimental evidence that **pseudothermal ghost imaging does not rely on nonlocal quantum correlations**. In addition, we show the depth-resolving capability of this ghost imaging technique.

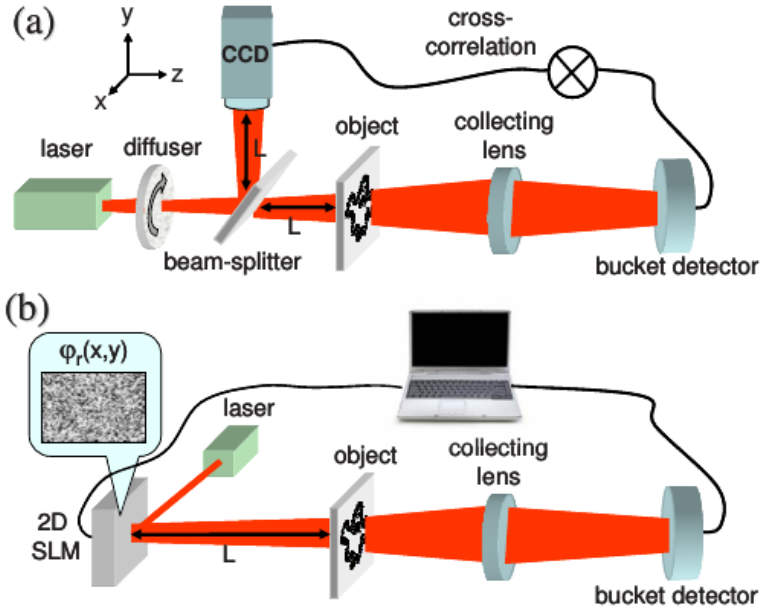

FIG. 1. (Color online) Experimental setups for ghost imaging. (a) The standard pseudothermal two-detector setup, where a ghost image of the object is obtained by correlating the pseudothermal field measured by a CCD with the intensity measured by a bucket detector. (b) The computational single-detector setup used in this work. A pseudothermal light beam is generated by applying controllable phase masks $\varphi_r(x,y)$ with a spatial light modulator (SLM). The object image is obtained by correlating the intensity measured by the bucket detector with the *calculated* field at the object plane.

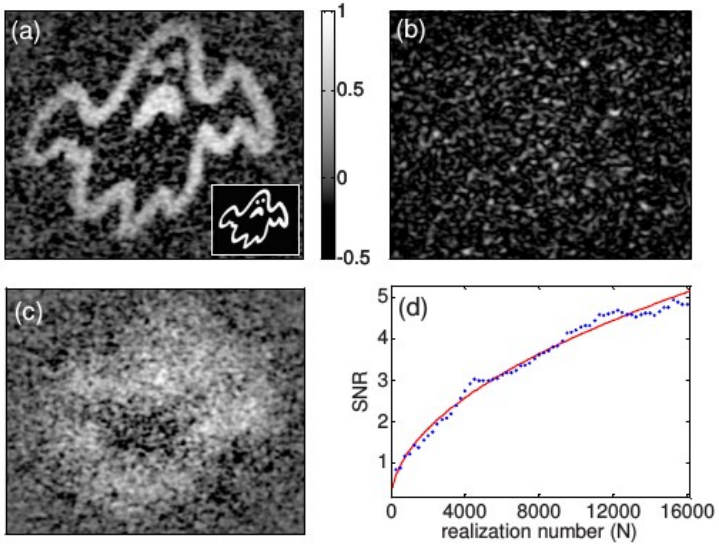

FIG. 2. (Color online) Computational ghost image reconstruction of a 2×2 cm^2 transmission mask placed at $L=84$ cm. (a) Reconstructed image at the object plane, obtained with 16 000 realizations. The inset shows the transmission mask. (b) A calculated intensity pattern of a single phase realization. The resolution of the reconstruction in (a) is dictated by the speckle size. (c) Reconstructed out-of-focus image, at a different z plane ($L=15$ cm), demonstrating the depth-resolving capabilities of the computational method. (d) Measured signal-to-noise ratio (SNR) of the reconstructed image as a function of the number of realizations (blue dots). The theoretical line depicts $\sqrt{N}$ dependence.

Idea detekcji punktowej obrazu (single-pixel detectors)

A New Compressive Imaging Camera Architecture using Optical-Domain Compression, D. Takhar et al., Proc. IS&T/SPIE Computational Imaging IV, 2006

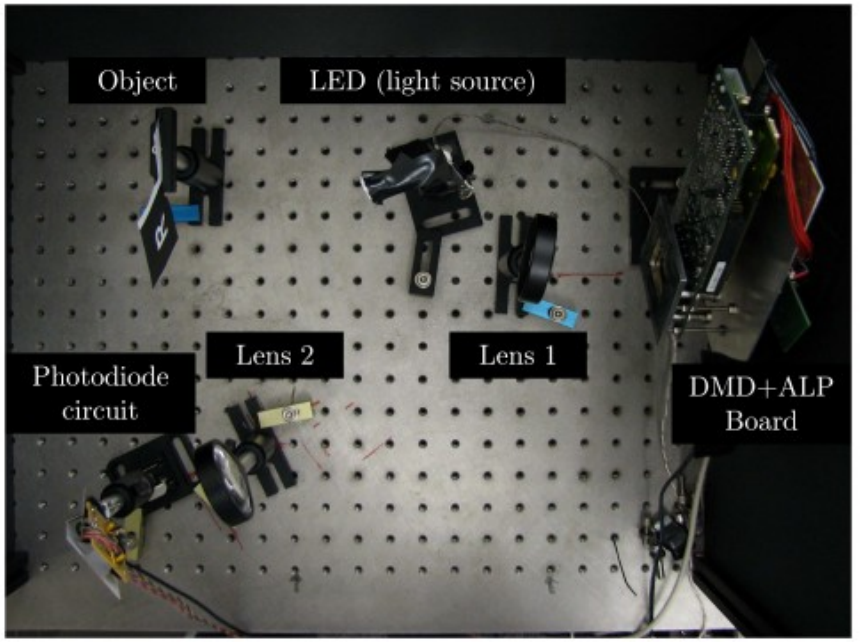

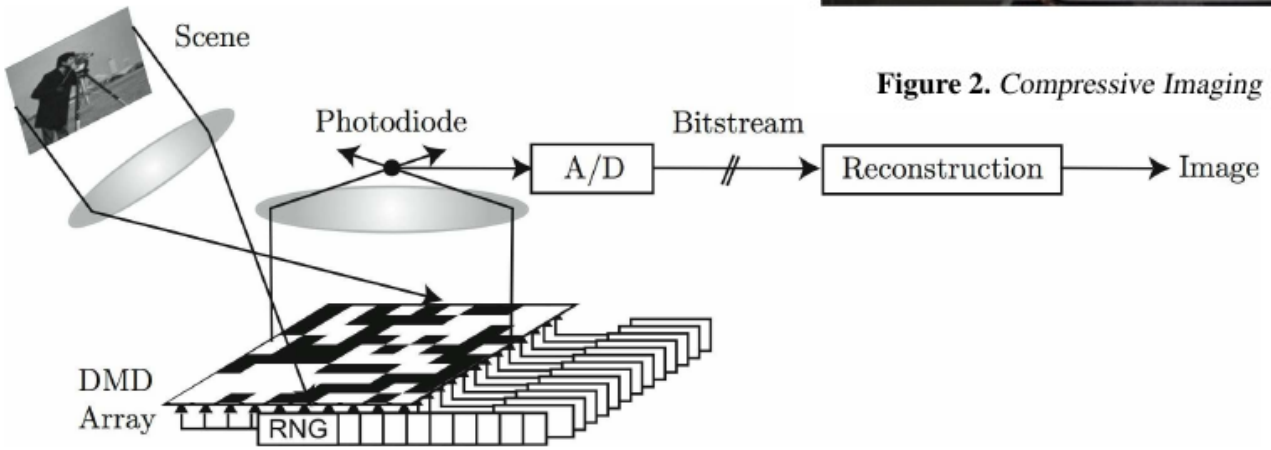

Figure 2. *Compressive Imaging (CI) camera hardware setup.*

Figure 1. *Compressive Imaging (CI) camera block diagram. Incident lightfield (corresponding to the desired image x) is reflected off a digital micro-mirror device (DMD) array whose mirror orientations are modulated in the pseudorandom pattern supplied by the random number generators (RNG). Each different mirror pattern produces a voltage at the single photodiode (PD) that corresponds to one measurement $y(m)$. From M measurements y we can reconstruct a sparse approximation to the desired image x using CS techniques.*

Idea detekcji punktowej obrazu (single-pixel detectors)

- **Single detector:** By time multiplexing a single detector, we can use a less expensive and yet more sensitive photon detector. This is particularly important when the detector is expensive, making an N-pixel array prohibitive. A single detector camera can also be adapted to image at wavelengths that are currently impossible with conventional CCD and CMOS imagers.
- **Universality:** Random and pseudorandom measurement bases are *universal* in the sense that they can be paired with any sparse basis. This allows exactly the same encoding strategy to be applied in a variety of different sensing environments; knowledge of the nuances of the environment are needed only at the decoder. Random measurements are also *future-proof*: if future research in image processing yields a better sparsity-inducing basis, then the same set of random measurements can be used to reconstruct an even better quality image.
- **Encryption:** A pseudorandom basis can be generated using a simple algorithm according to a random seed. Such encoding effectively implements a form of *encryption*: the randomized measurements will themselves resemble noise and be meaningless to an observer who does not know the associated seed.
- **Robustness and progressivity:** Random coding is robust in that the randomized measurements have equal priority, unlike the Fourier or wavelet coefficients in current transform coders. Thus they allow a *progressively better reconstruction* of the data as more measurements are obtained; one or more measurements can also be lost without corrupting the entire reconstruction.
- **Scalability:** We can adaptively select how many measurements to compute in order to trade off the amount of compression of the acquired image versus acquisition time; in contrast, conventional cameras trade off resolution versus the number of pixel sensors.
- **Computational asymmetry:** Finally, CI places most of its computational complexity in the decoder, which will often have more substantial computational resources than the encoder/imager. The encoder is very simple; it merely computes incoherent projections and makes no decisions.

MIT Technology Review

NEWS & ANALYSIS ▾ | FEATURES | VIEWS | MULTIMEDIA | DISCUSSIONS | TOPICS | POPULAR: 10 BREAKTHROUGH TE

VIEW

6 COMM

Emerging Technology From the arXiv

June 3, 2013

Bell Labs Invents Lensless Camera

A new class of imaging device with no lens and just a single light sensitive sensor could revolutionise optical, infrared and millimetre wave imaging

http://www.technologyreview.com/view/515651/bell-labs-invents-lensless-camera/

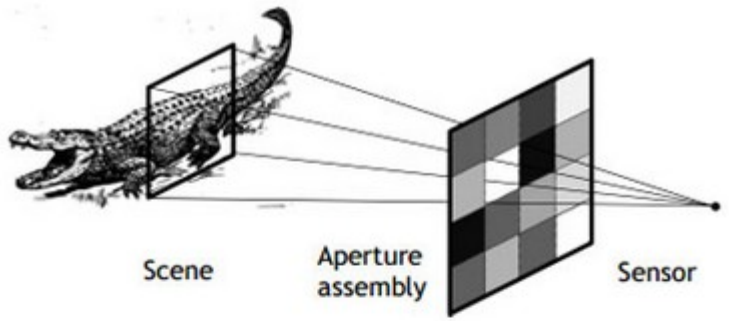

Przykład: kolorowa kamera o “nieograniczonej” głębi ostrości, bez obiektywu i bez macierzy detektorów (wykorzystany jest pojedynczy detektor, modulator przestrzenny i filtry dla barw podstawowych; można łatwo zmienić zakres widmowy np. do zakresu THz)

Connectivity

New Camera Can See Around Corners

Chinese scientists have built a camera capable of photographing objects it can't directly see.

by Emerging Technology from the arXiv January 6, 2017

In the last few years, single-pixel cameras have begun to revolutionize the field of imaging. These counterintuitive devices produce high-resolution images using a single pixel to detect light. They do not need lenses, the images of have none of the distortions that lenses produce, and the entire picture is always in focus. Physicists have used them to make movies and even to create 3-D images.

And that raises an interesting question: how much more can these devices do?

Today we get an answer of sorts thanks to the work of Bin Bai and co at Xi'an Jiaotong University in China, who have built a single pixel camera that can see around corners. Their new device can photograph objects even when they are not in direct view.

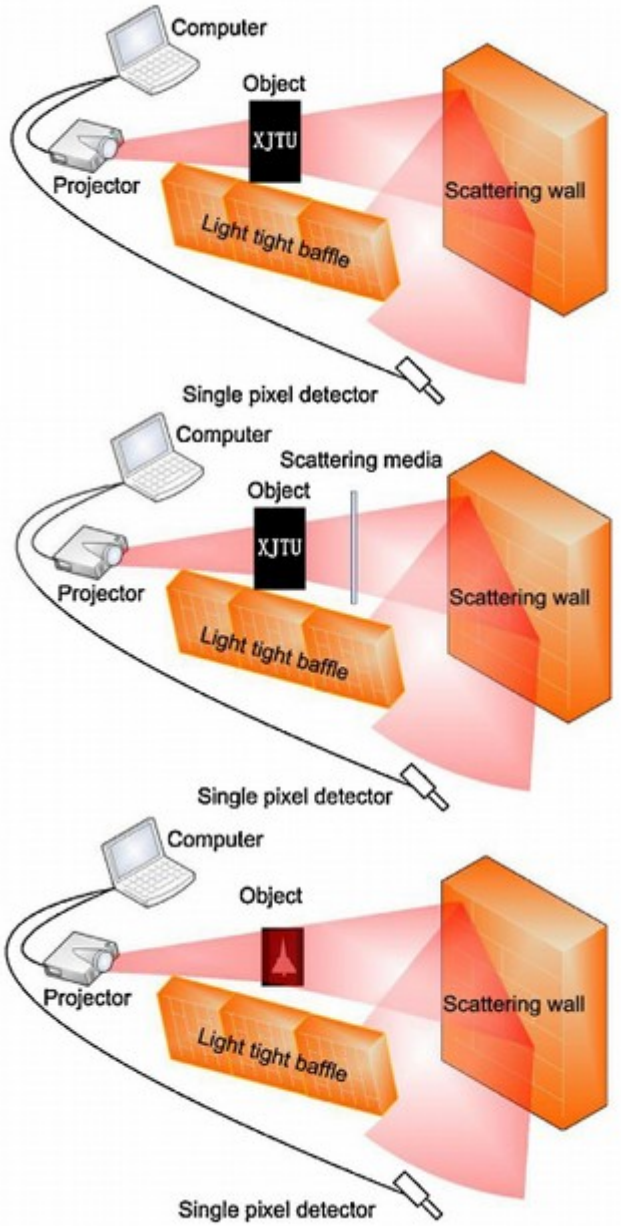

Optik147(2017)136–142

Konstrukcja kamery na podczerwień

R. M. Willett et al, Compressed sensing for practical optical imaging systems: a tutorial, Opt. Eng. 50, 072601, 2011

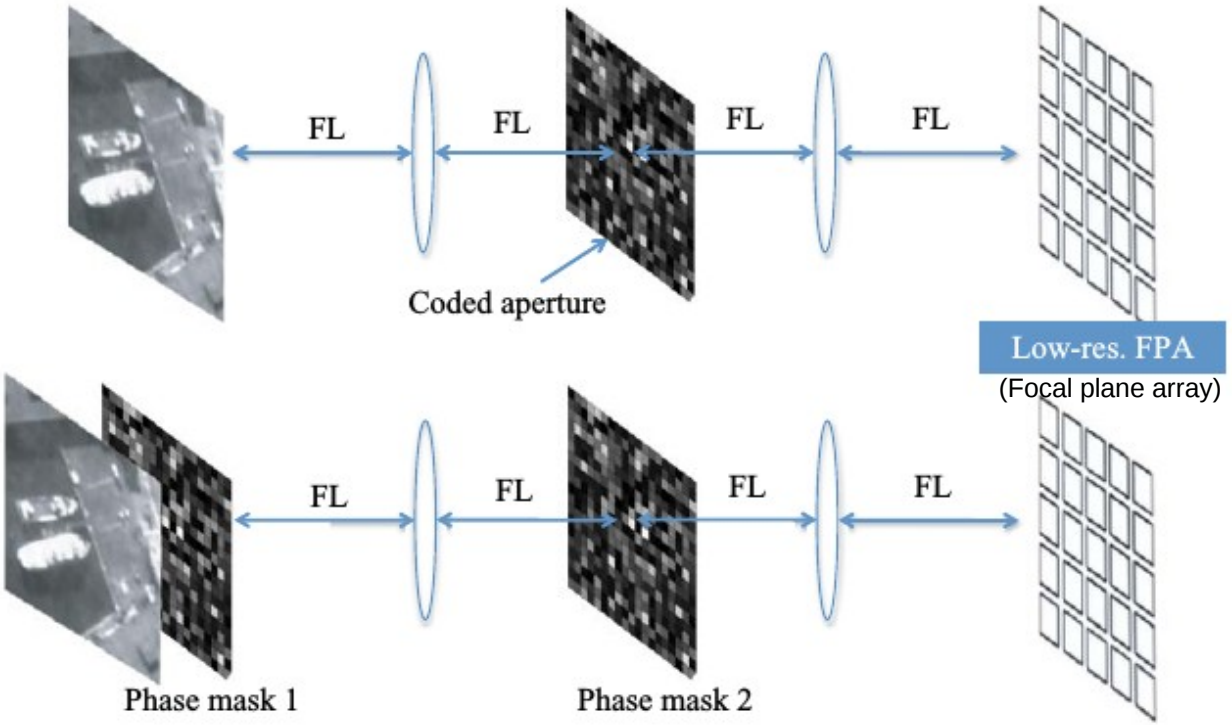

(a)

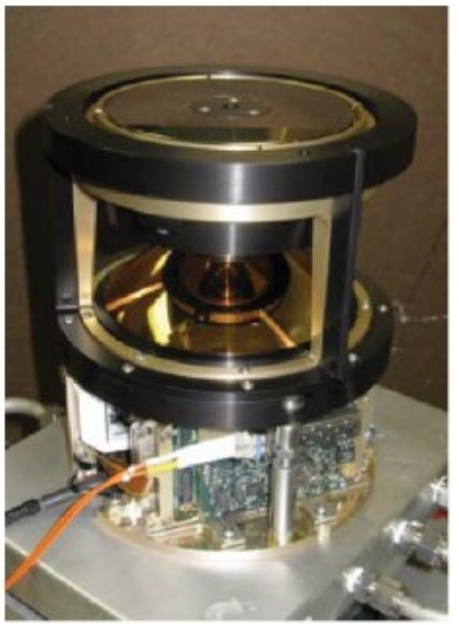

(b)

Fig. 3 Infrared camera examples. (a) Two possible IR camera architectures. In the first, a coded aperture is placed in the lens Fourier plane, while in the second, two different phase masks are used to create the measurement matrix. (b) Panoramic midwave camera assembly.

3D Computational Imaging with Single-Pixel Detectors

Przykład: obrazowanie 3D z 4 detektorami punktowymi

B. Sun,[1*] M. P. Edgar,[1] R. Bowman,[1,2] L. E. Vittert,[3] S. Welsh,[1] A. Bowman,[3] M. J. Padgett[1]

Computational imaging enables retrieval of the spatial information of an object with the use of single-pixel detectors. By projecting a series of known random patterns and measuring the backscattered intensity, it is possible to reconstruct a two-dimensional (2D) image. We used several single-pixel detectors in different locations to capture the 3D form of an object. From each detector we derived a 2D image that appeared to be illuminated from a different direction, even though only a single digital projector was used for illumination. From the shading of the images, the surface gradients could be derived and the 3D object reconstructed. We compare our result to that obtained from a stereophotogrammetric system using multiple cameras. Our simplified approach to 3D imaging can readily be extended to nonvisible wavebands.

Science 340, 844 (2013);
DOI: 10.1126/science.1234454

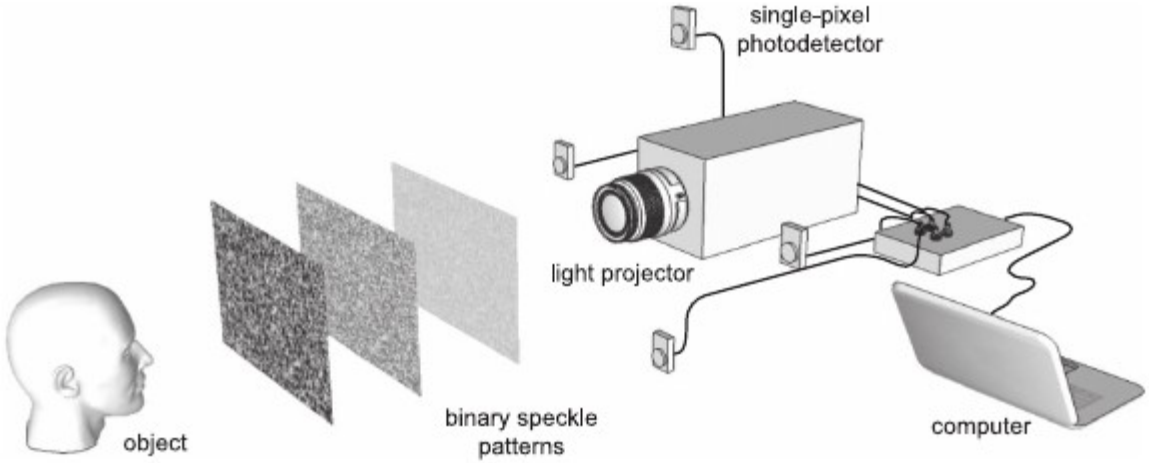

Fig. 1. Experimental setup used for 3D surface reconstructions. The light projector illuminates the object (head) with computer-generated random binary speckle patterns. The light reflected from the object is collected on four spatially separated single-pixel photodetectors. The signals from the photodetectors are measured and used to reconstruct a computational image for each photodetector.

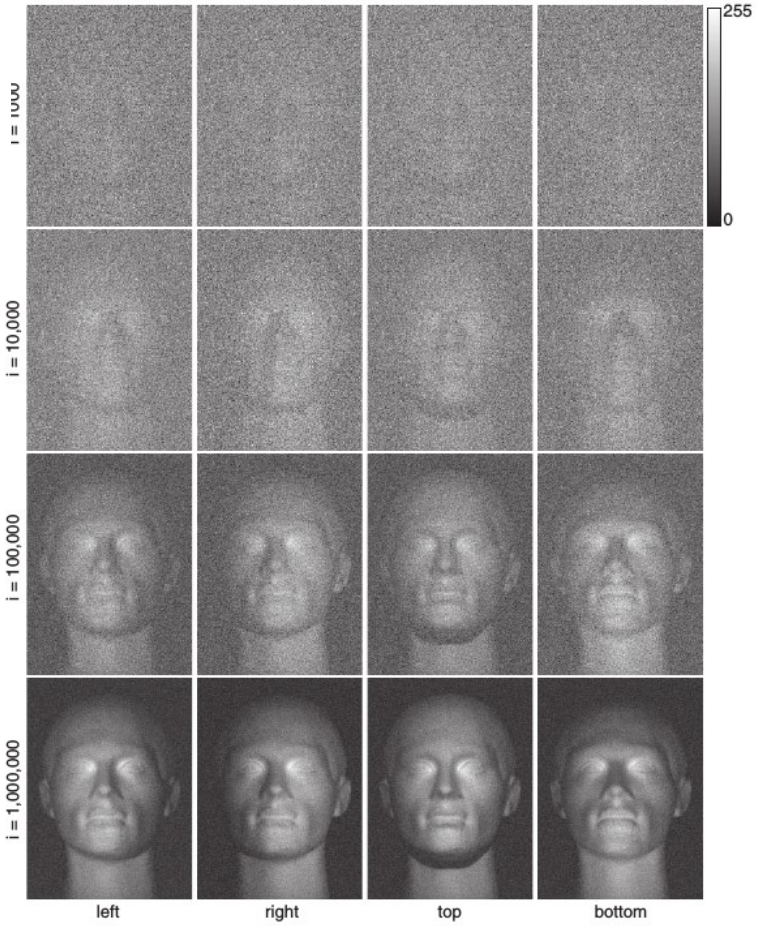

Fig. 2. Source images from the four single-pixel detectors from 1000 to 1 million iterations. The images from each photodetector are reconstructed using an iterative algorithm (described in the text). The spatial information in each image is identical; however, the apparent illumination source is determined by the location of the relevant photodetector, indicated underneath. No postprocessing has been applied to the images. The scale refers to the relative intensity of the images (in arbitrary units, 0 to 255).

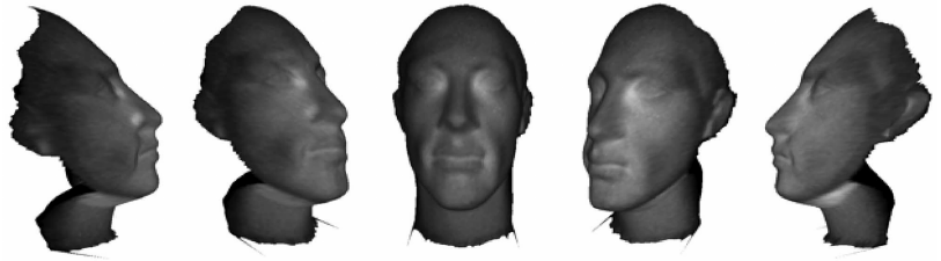

Fig. 3. 3D reconstruction of the object. Rendered views of the reconstructed facial surface derived by integration of the surface normal data and overlaid with the reflectivity data (see movie S1).

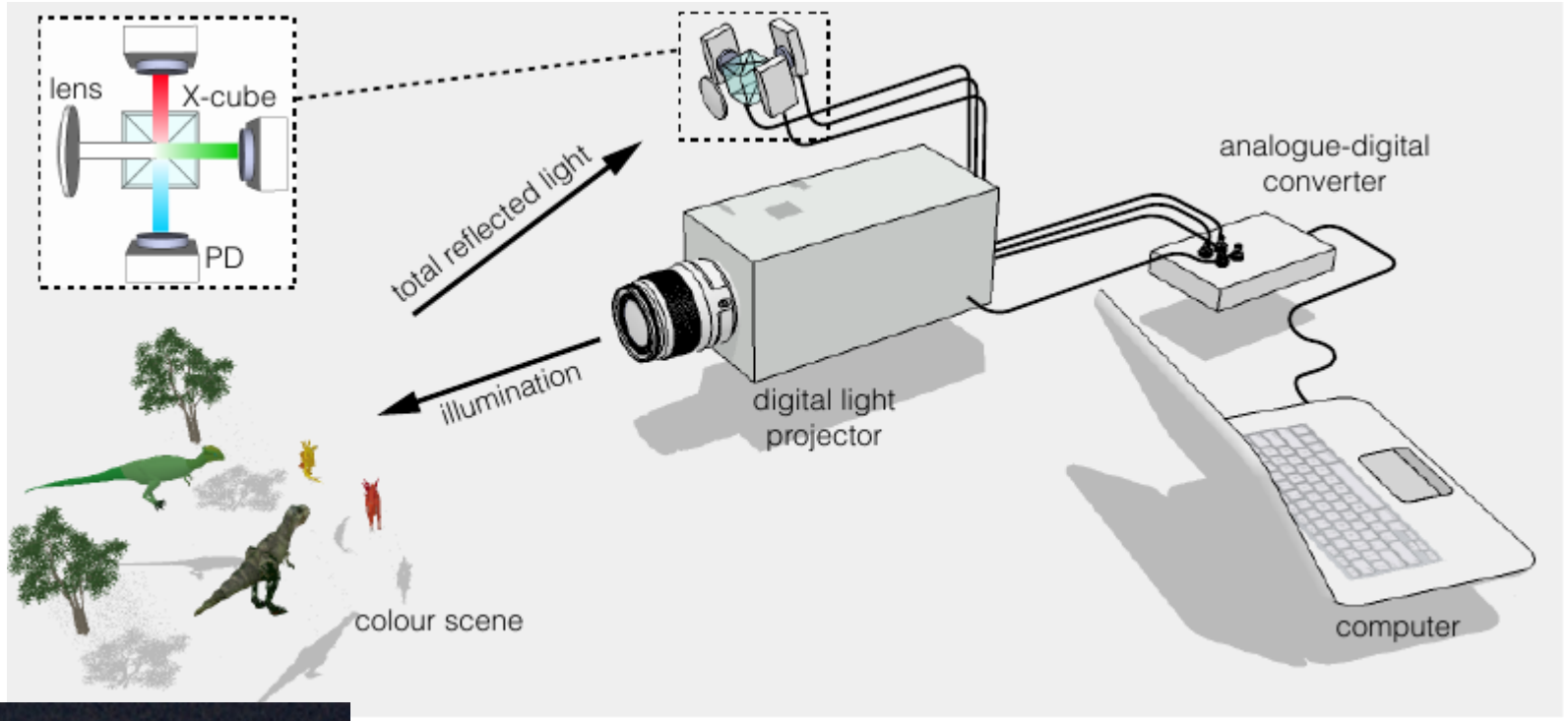

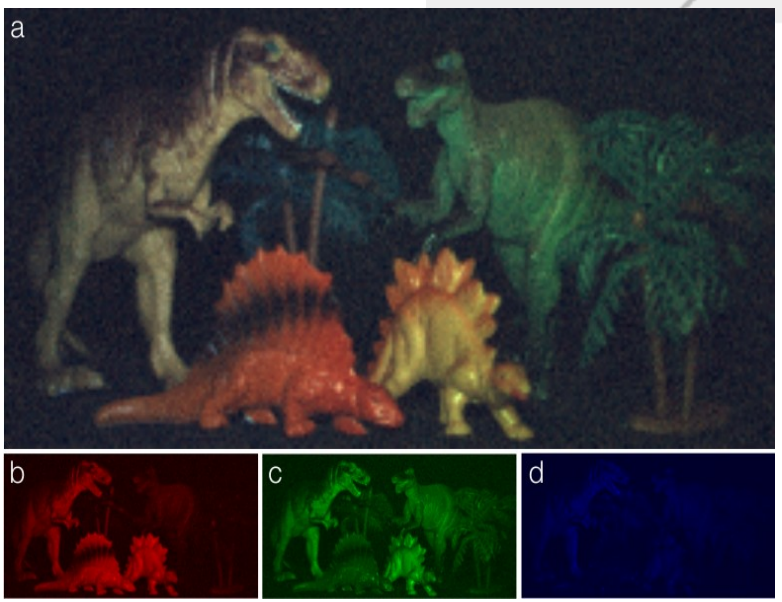

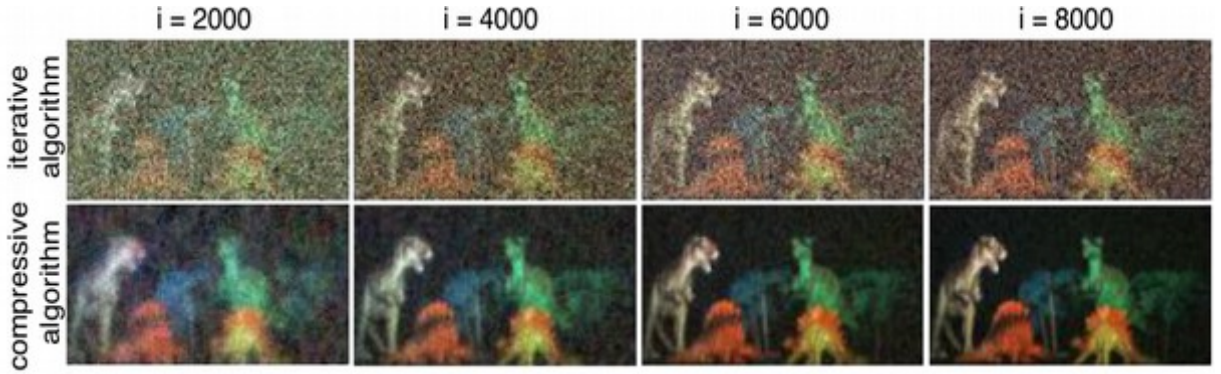

Welsh et al, “Fast full-color computational imaging with single-pixel detectors”
Opt. Express 21, 2013, DOI:10.1364/OE.21.023068

Texas Instruments DLP 4500

http://www.ti.com/lit/ug/dlpu011d/dlpu011d.pdf

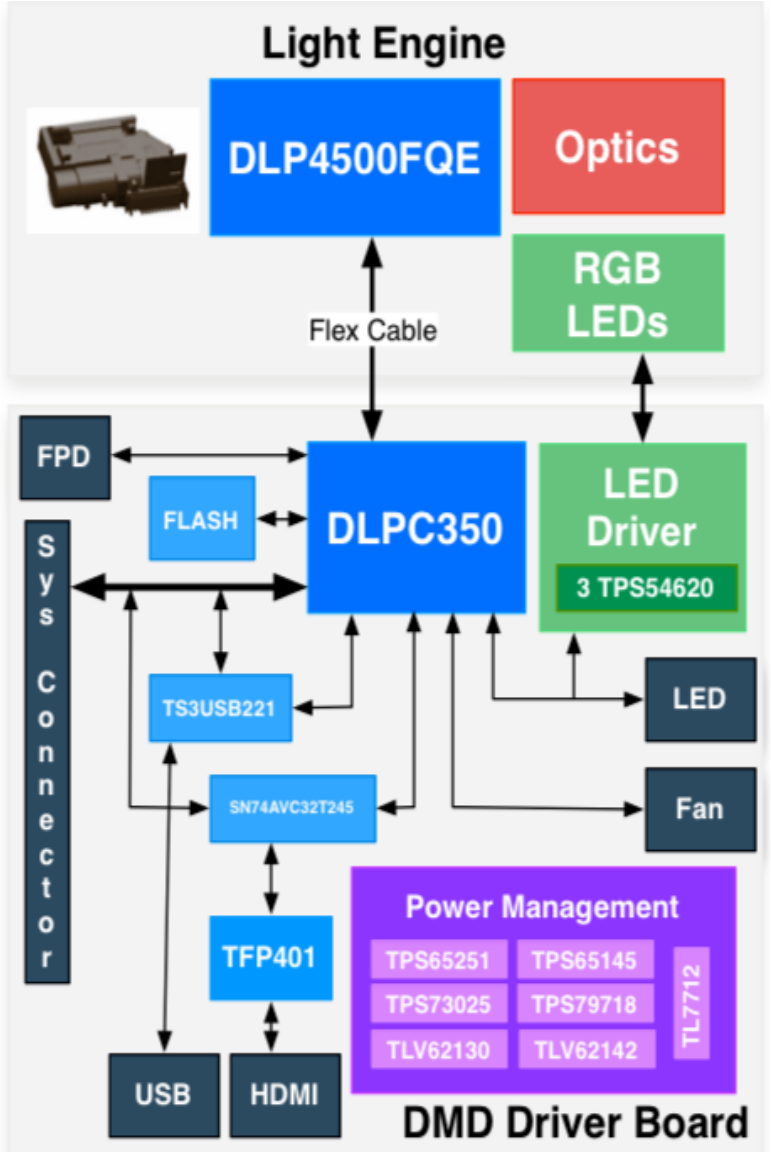

- Structured light applications:
  - 3D modeling and design
  - Fingerprint identification
  - Face recognition
  - Machine vision and inspection
- Medical and life sciences:
  - Vascular imaging
  - Dental impression scanners
  - Intraoral dental scanners
  - Orthopedics, prosthesis, CT, MRI, and X-ray marking
  - Retail cosmetics
- Small display projectors:
  - Embedded display
  - Interactive display
  - Information overlay
- TI NIRscan EVM
  - TI NIRscan EVM has many similarites with the LightCrafter 4500 module
  - NIRscan uses the DLP4500 DMD in structured light mode to provide a cheap, efficient spectroscopy solution
  - For more information visit NIRscan page on the TI website

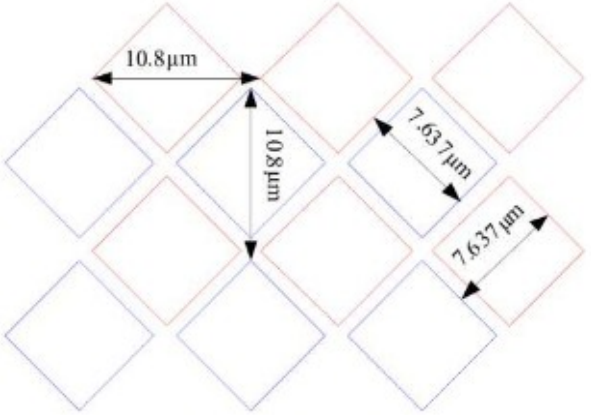

Figure 1-3. 0.45-Inch DMD Diamond Pixel Geometry

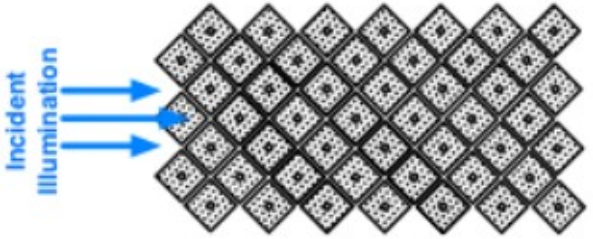

Figure 1-4. 0.45-Inch DMD Diamond Pixel Array Configuration

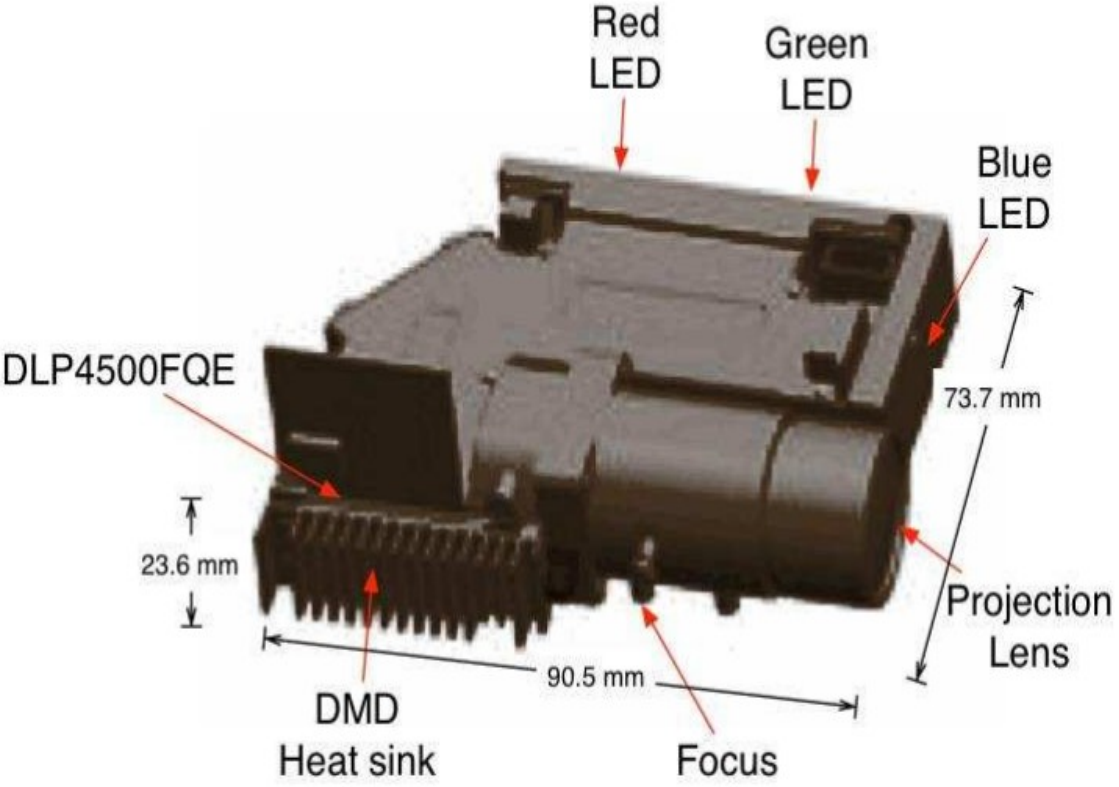

Figure 1-2. iView Light Engine

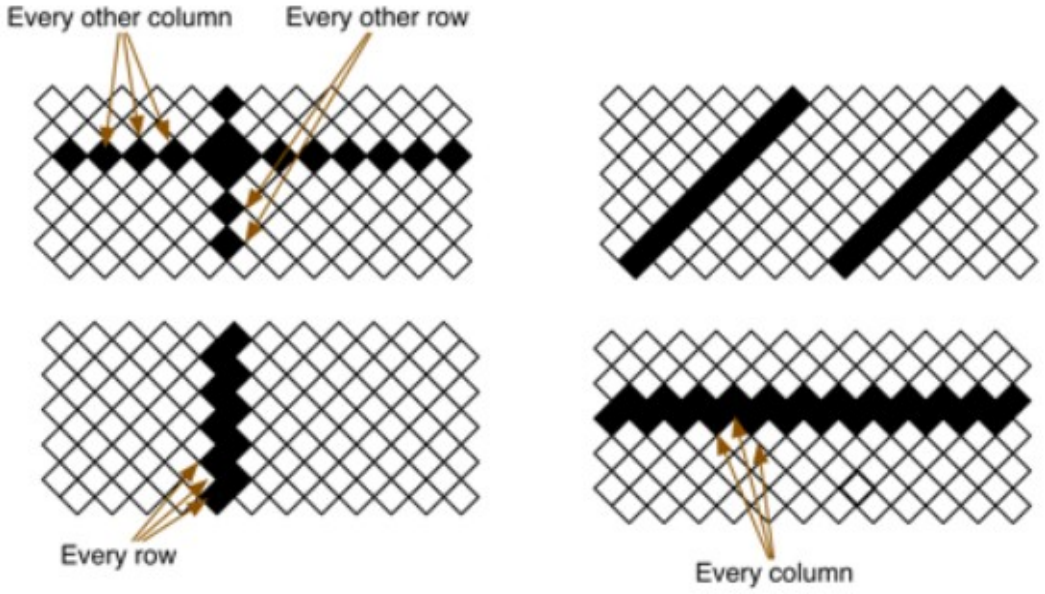

Figure 1-5. Diamond Pixel for Vertical, Horizontal, and Diagonal Lines

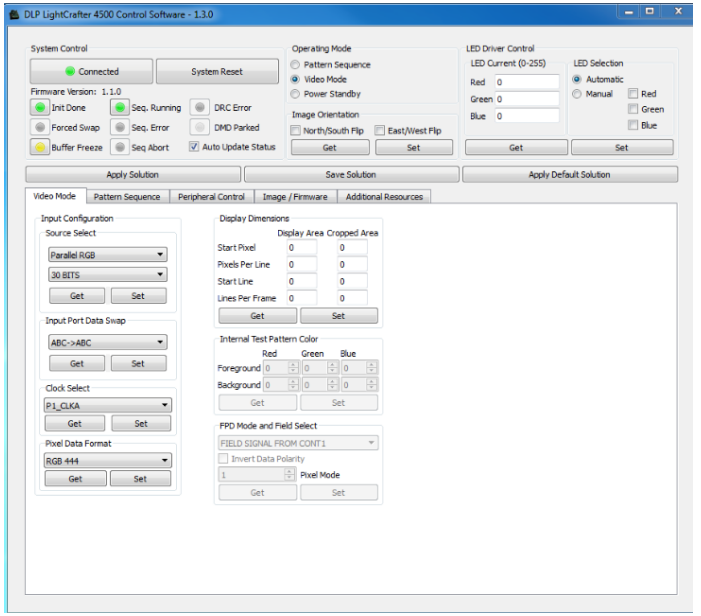

Zhao et al, **Ghost imaging lidar** via sparsity constraints, Appl. Phys. Lett. 101,141123 (2012); doi: 10.1063/1.4757874

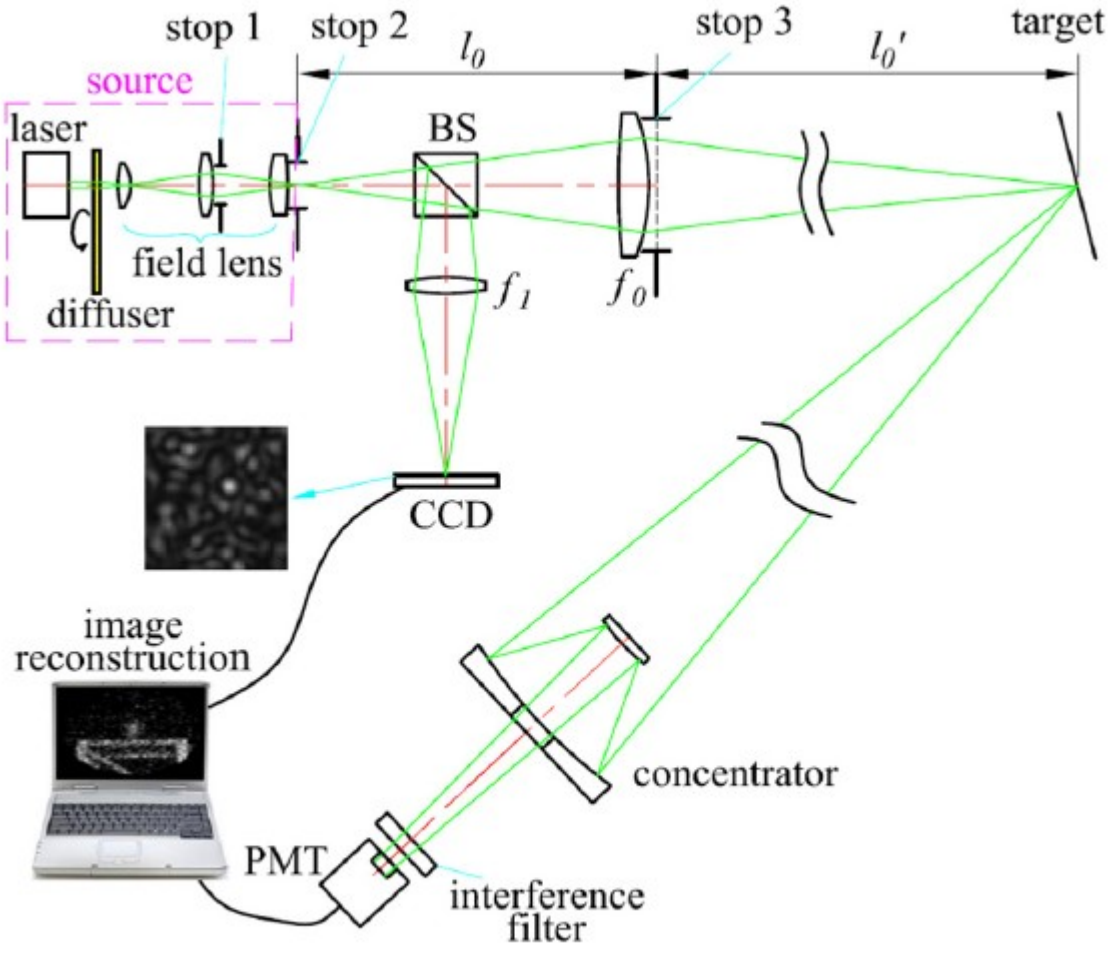

FIG. 1. Experimental setup of GISC lidar.

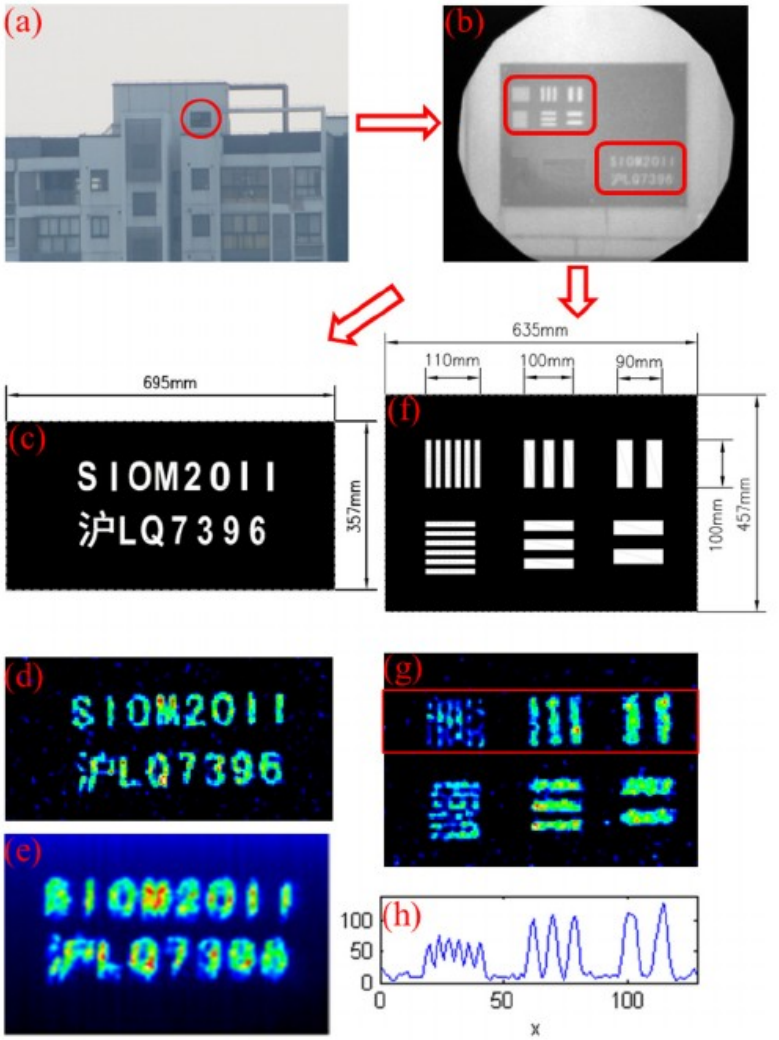

FIG. 2. Experimental reconstruction results for high-reflection targets we proposed at 900 m range (with $M = 3000$ measurements). (a) and (b) The original target plates imaged by a camera and a telescope, respectively; (c) the concrete sizes of a standard Chinese vehicle license plate; (f) the concrete sizes of a set of resolution panels; (d) and (g) are the targets' images reconstructed by GISC lidar and the targets are all represented in the space basis; (e) the imaging result obtained by replacing the PMT with a camera in Fig. 1 and accumulating 3000 measurements (the receiving aperture of telescope is 420 mm); (h) the cross-section of the rectangular selection box in (g).

Ladar- radar laserowy

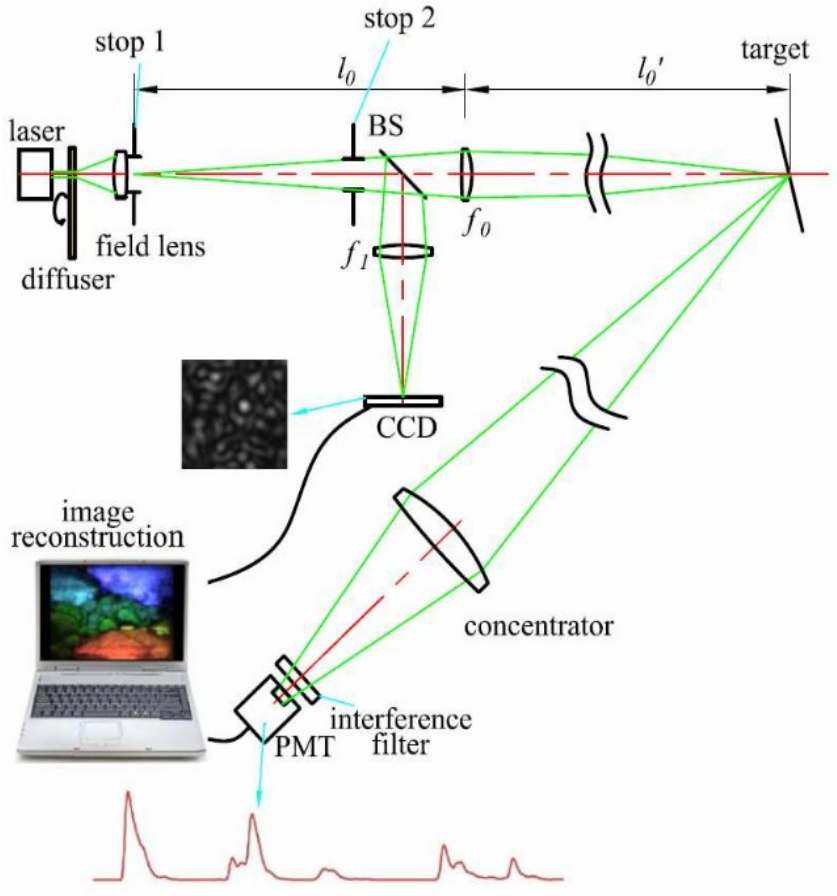

FIG. 1: Experimental setup of 3D GI ladar system with pseudo-thermal light.

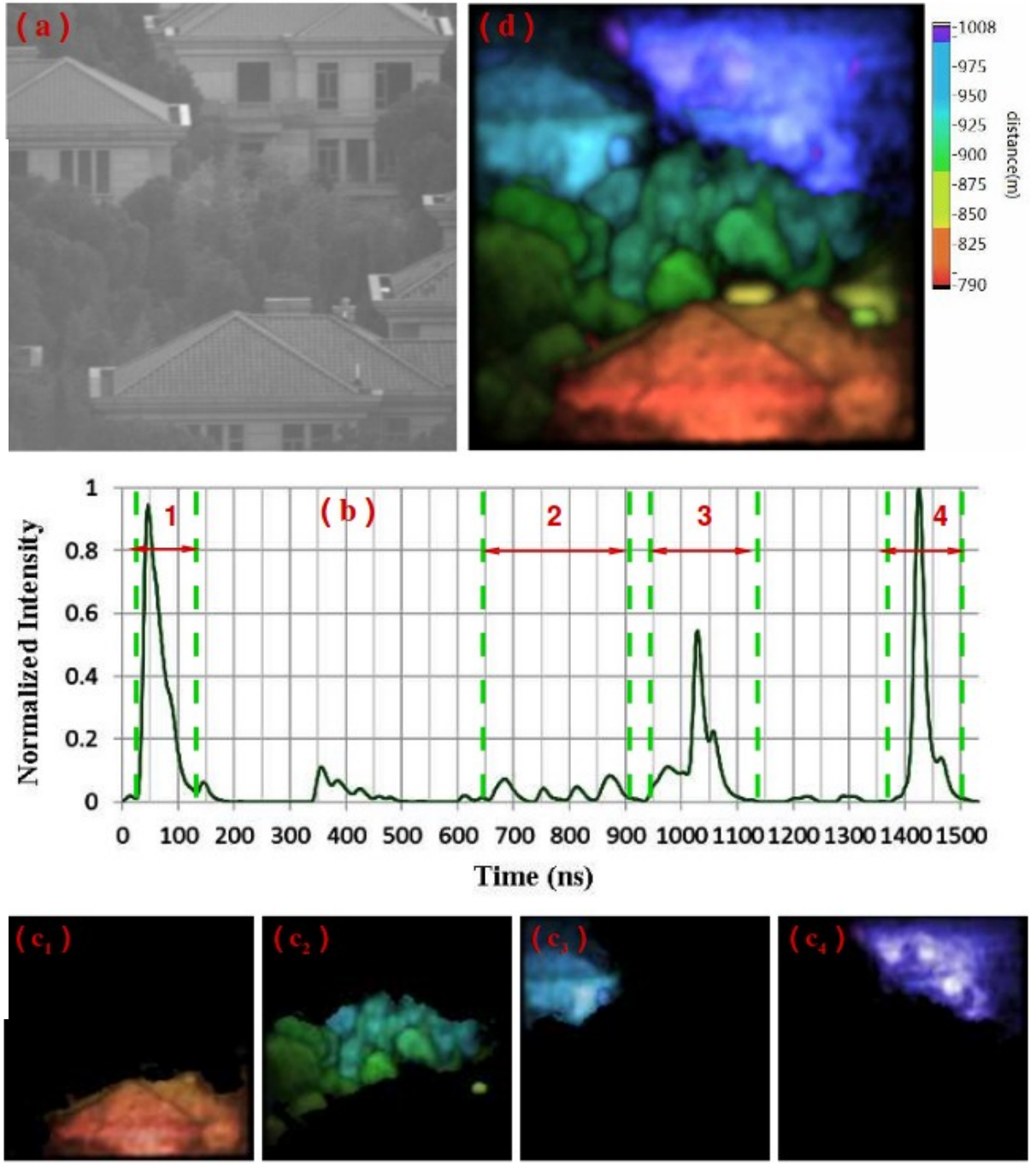

Three-dimensional ghost imaging ladar, Gong et al. 2013

http://arxiv.org/pdf/1301.5767v1.pdf

FIG. 4: Experimental demonstration results of a large imaging scene located about l_0'=900 m away, the captions ar

as Fig. 2 and Fig. 3.

Nadrozdzielczość + pomiar informacji fazowej

Super-resolution and reconstruction of sparse sub-wavelength images,
Gazit et al., Opt. Express 2009

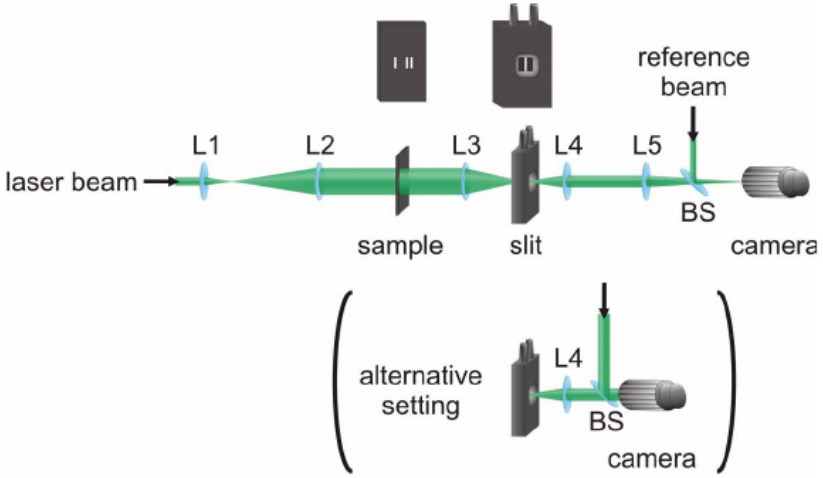

Fig. 3. **Experimental setup for the proof-of-concept experiments.** The laser beam is collimated using lenses L1 and L2, before the sample is illuminated. The signal is then Fourier transformed using lens L3, low-pass filtered by the slit and again Fourier transformed into the real plane by lens L4. Another lens L5 performs an additional Fourier transform, which is recorded by a camera. In order to measure the phase distribution, a probe beam is superimposed (using the beam splitter BS) on the signal in order to create interference fringes. In an alternative setup, the information can be directly taken in the real plane, so that the camera is positioned directly behind lens L4. .

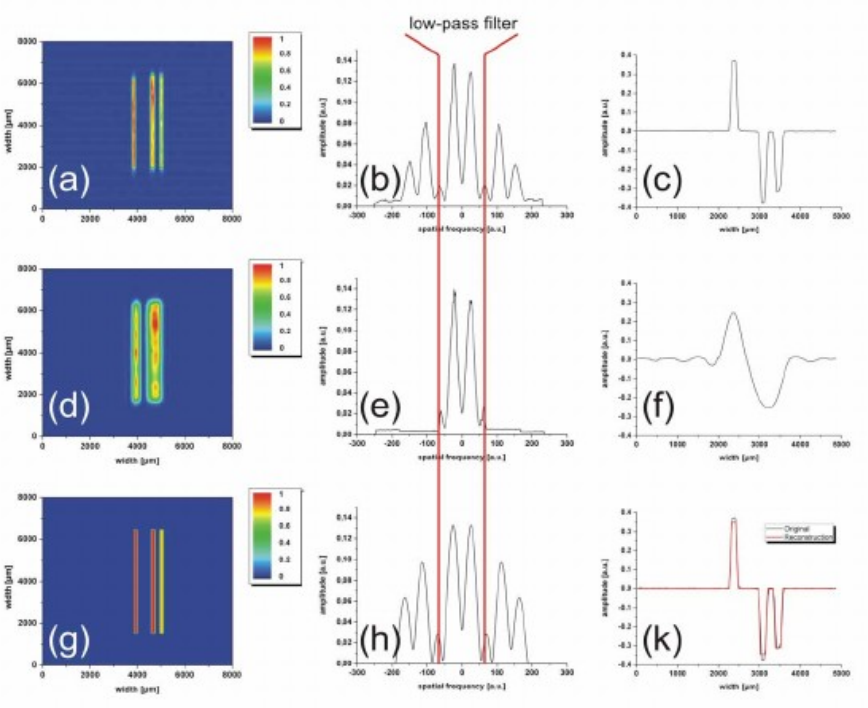

Fig. 5. **Experimental proof-of-concept: reconstruction of amplitude + phase information.** An important feature of our proposed algorithm is the ability to recover both amplitude and phase, which is essential for pictorial information carried upon electromagnetic waves. (a,b,c) The original information consisting of three vertical stripes (a), its Fourier spectrum (b), and a horizontal cross-section of the amplitude, taken through the real-space information, revealing that the two stripes on the right are π-phase shifted with respect to the stripe on the left (c). (d,e,f) Using the optical slit, the signal is low-pass filtered at the vertical red lines, yielding a highly blurred image consisting of two distinct lobes (d). The Fourier spectrum now contains now only the lowest frequencies (e), which cause the mergence of the two stripes on the right, as seen in the horizontal cross section (f). (g,h,k) Reconstruction using CS methods yields a high quality recovered information (g) and its respective Fourier spectrum (h). The strong correspondence between original and recovery is clearly visible in the horizontal cross section (k).

Mikroskopia fluorescencyjna

Compressive fluorescence microscopy for biological and hyperspectral imaging,
V. Studera, PNAS 2012,
doi:10.1073/pnas.1119511109

The mathematical theory of compressed sensing (CS) asserts that one can acquire signals from measurements whose rate is much lower than the total bandwidth. Whereas the CS theory is now well developed, challenges concerning hardware implementations of CS-based acquisition devices—especially in optics—have only started being addressed. This paper presents an implementation of compressive sensing in fluorescence microscopy and its applications to biomedical imaging. Our CS microscope combines a dynamic structured wide-field illumination and a fast and sensitive single-point fluorescence detection to enable reconstructions of images of fluorescent beads, cells, and tissues with undersampling ratios (between the number of pixels and number of measurements) up to 32. We further demonstrate a hyperspectral mode and record images with 128 spectral channels and undersampling ratios up to 64, illustrating the potential benefits of CS acquisition for higher-dimensional signals, which typically exhibits extreme redundancy. Altogether, our results emphasize the interest of CS schemes for acquisition at a significantly reduced rate and point to some remaining challenges for CS fluorescence microscopy.

Compressive Fluorescence Microscopy: Implementation

Experimental Setup. Our setup is based on a standard epifluorescence inverted microscope (Nikon Ti-E) as shown in Fig. 1*A*. To generate spatially modulated excitation patterns, we incorporated a Digital Micromirror Device (DMD) in a conjugate image plane of the excitation path. The DMD is a 1,024-by-768 array of micromirrors (Texas-Instrument Discovery 4100) of size 13.68 × 13.68 μm each, and which can be shifted between two positions oriented at +12° or −12° with respect to the DMD surface. The

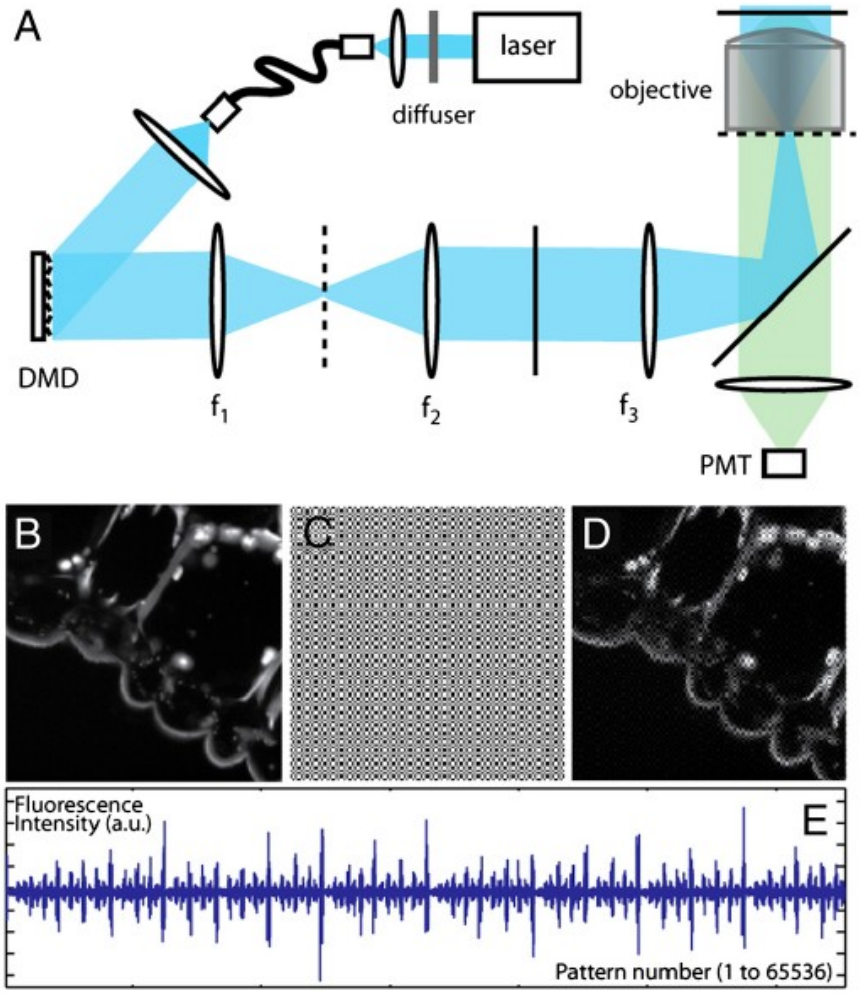

Fig. 1. (*A*) Experimental setup. The dotted and plain segments correspond to planes respectively conjugated to the pupil and sample planes. (*B*) Slice of lily anther (endogenous fluorescence with epifluorescence microscopy image recorded on a CCD camera). (*C*) Projection of a Hadamard pattern on a uniform fluorescent sample. (*D*) Projection of the same Hadamard pattern on the biological sample. (*E*) Fluorescence intensity during an acquisition sequence.

Lensfree Fluorescent On-Chip Imaging Using Compressive Sampling
A. F. Coskun et al. Opt. Photon News, Dec 2010

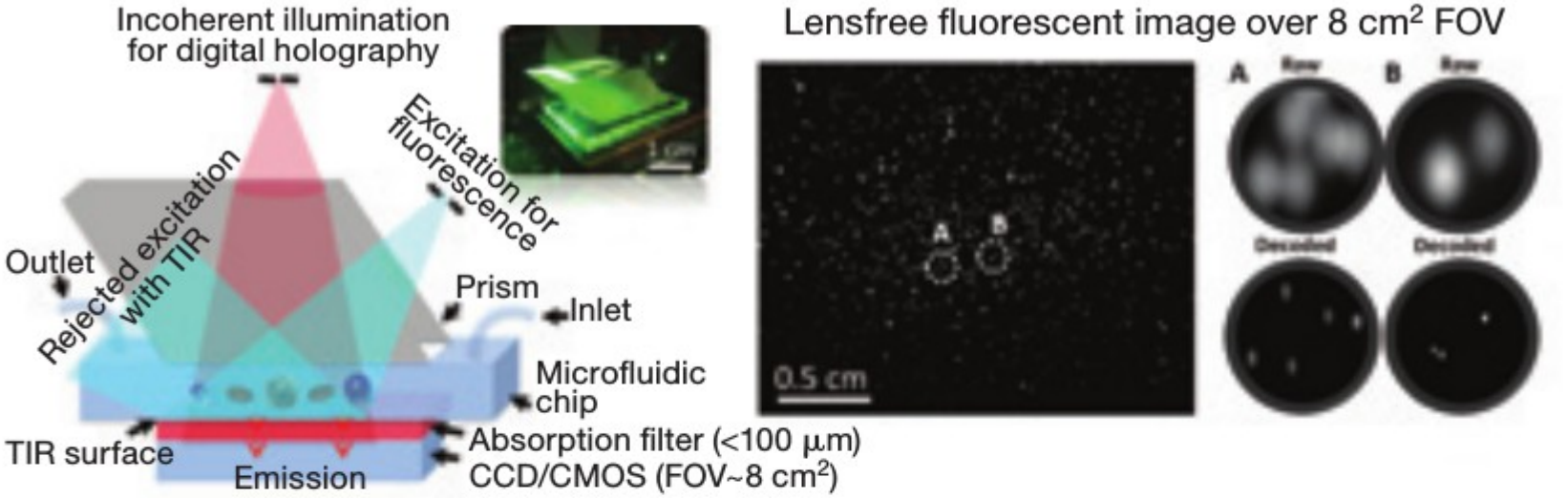

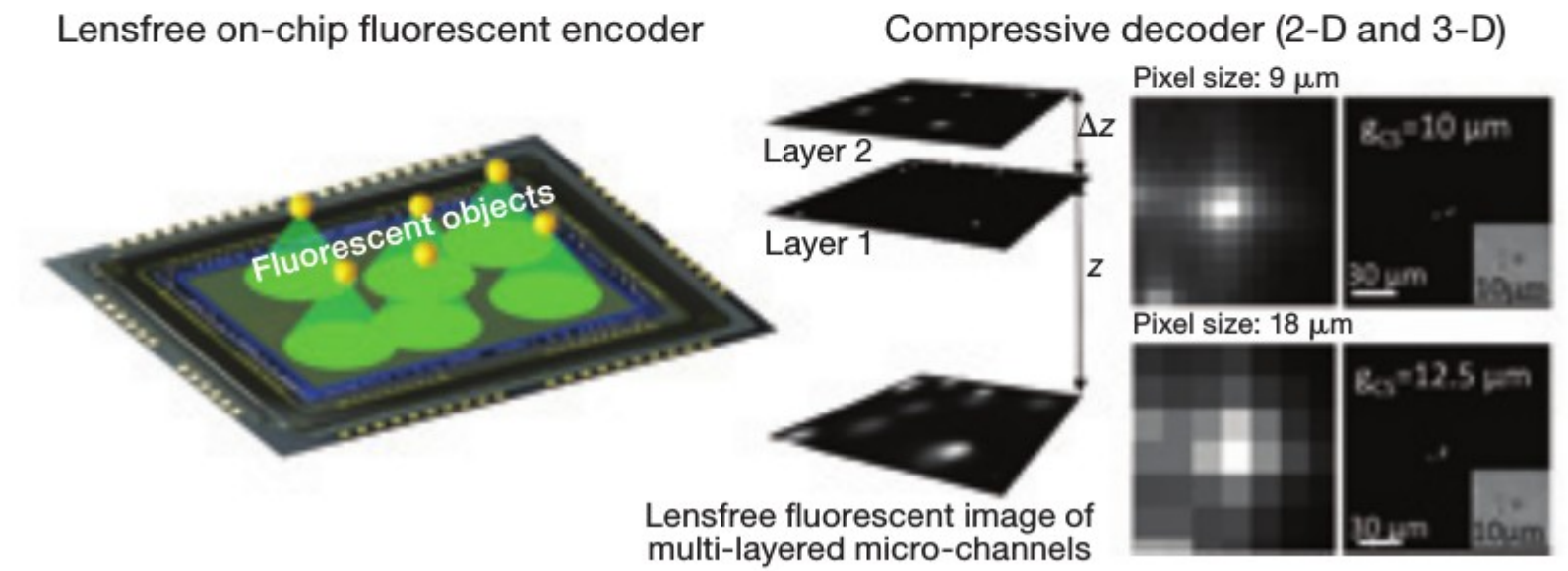

Terahertz imaging with compressed sensing

Chan et al, Opt. Lett,33,974, 2008

We describe a novel, high-speed pulsed terahertz (THz) Fourier imaging system based on compressed sensing (CS), a new signal processing theory, which allows image reconstruction with fewer samples than traditionally required. Using CS, we successfully reconstruct a 64×64 image of an object with pixel size 1.4 mm using a randomly chosen subset of the 4096 pixels, which defines the image in the Fourier plane, and observe improved reconstruction quality when we apply phase correction. For our chosen image, only about 12% of the pixels are required for reassembling the image. In combination with phase retrieval, our system has the capability to reconstruct images with only a small subset of Fourier *amplitude* measurements and thus has potential application in THz imaging with cw sources.

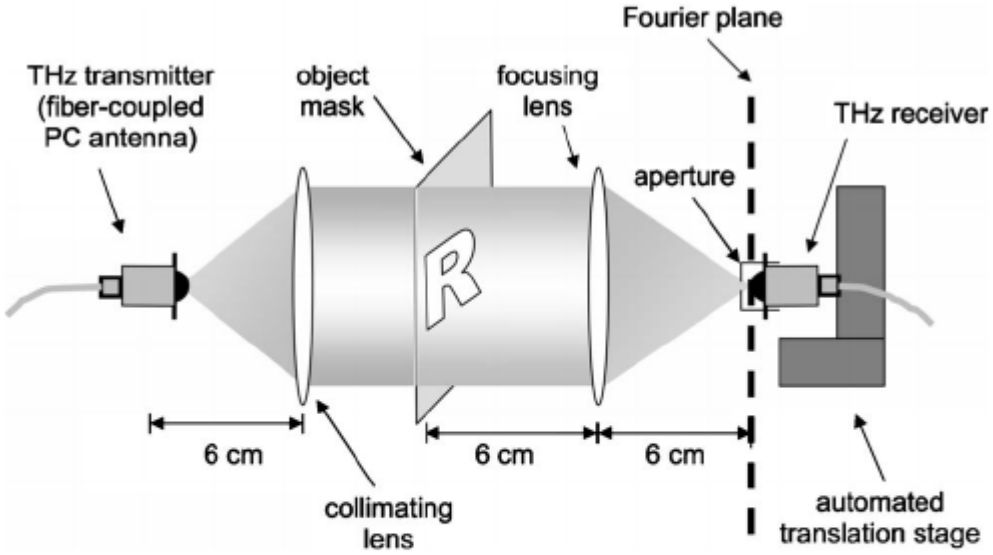

Fig. 1. THz Fourier imaging setup. An approximately collimated beam from the THz transmitter illuminates an object mask, placed one focal length away from the focusing lens. The THz receiver raster scans and samples the Fourier transform of the object on the focal plane.

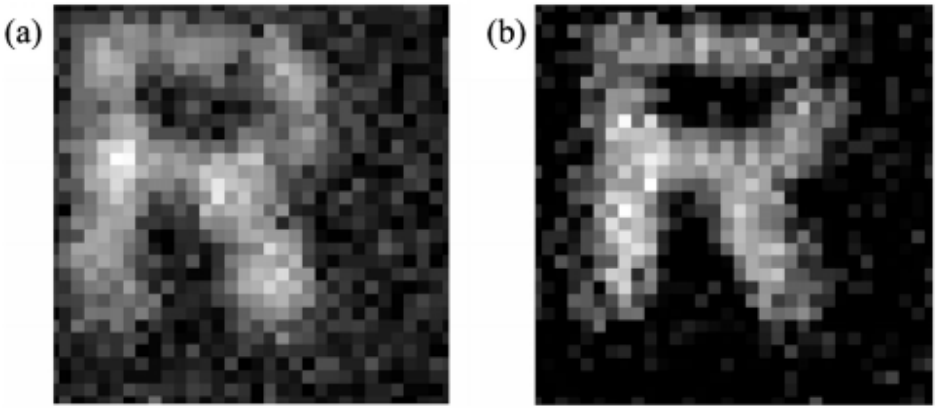

Fig. 3. Image reconstruction results using (a) CPR with the full dataset (4096 magnitude measurements) and (b) CSPR with a subset of 1500 measurements from the dataset used in (a).

Zastosowania w sejsmologii

A compressive sensing framework for seismic source parameter estimation, I. Rodriguez et al., Geophys. J. Int. (2012), doi: 10.1111/j.1365-246X.2012.05659.x

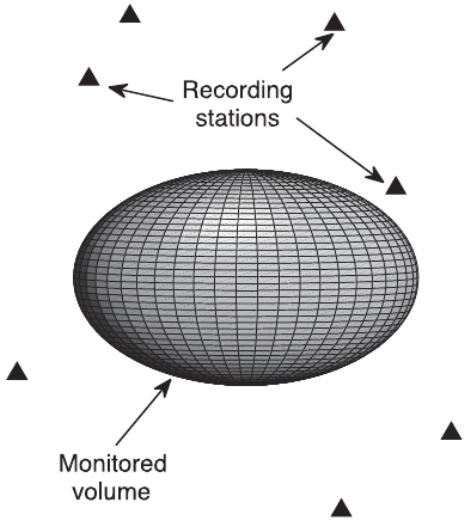

Figure 1. Diagram of the seismic event monitoring setting. The monitored volume (grid) encloses a region with potential seismic activity.

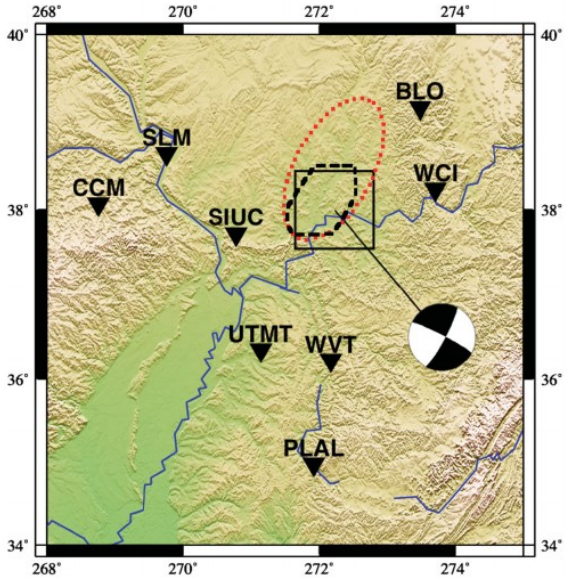

Figure 8. Distribution of recording stations considered in the inversion tests for the 2002 June 18 Caborn earthquake (black triangles). The black square represents the surface projection of the monitoring grid. The dotted line delimits the WVSZ, and the dashed line the WVFS. The beach ball representation corresponds to the solution determined by Kim (2003) joined by a line to its epicentral location. Image after Vera Rodriguez *et al.* (2012).

Table 1. Comparison of different solutions for the June 18, Caborn earthquake. NNA stands for the number of non-adaptive measurements per non-zero coefficient in the CS solution. DS stands for dictionary size after compression, where 100 per cent corresponds to the uncompressed dictionary. Success rate refers to the percentage of times that the event was detected using the CS approach in 500 realizations of sensing matrix.

Solution	Success rate (per cent)	Origin time 17 hr 37 min + (s)	Location	Source mechanism
Kim (2003)	N/A	17.2	37.99° N 87.77° W Depth (18 ± 2) km	
Vera Rodriguez *et al.* (2012)	N/A	16.0	37.988° N 87.770° W Depth 20.5 km	
NNA = 5 DS = 0.7 per cent	4.6	16.0 ± 0.2	(37.988 ± 0.000)° N (87.770 ± 0.000)° W Depth (18.98 ± 2.35) km	
NNA = 20 DS = 2.8 per cent	31.4	16.0 ± 0.0	(37.988 ± 0.000)° N (87.770 ± 0.000)° W Depth (20.21 ± 1.17) km	
CS				
NNA = 40 DS = 5.6 per cent	60.0	16.0 ± 0.0	(37.988 ± 0.000)° N (87.770 ± 0.000)° W Depth (20.47 ± 0.41) km	
NNA = 120 DS = 16.7 per cent	96.8	16.0 ± 0.0	(37.988 ± 0.000)° N (87.770 ± 0.000)° W Depth (20.50 ± 0.00) km	

Idea działania CS - pomiar

Kompresowalność sygnału x:

The signal x is *K-sparse* if it is a linear combination of only K basis vectors; that is, only K of the s_i coefficients in (1) are nonzero and $(N - K)$ are zero. The case of interest is when $K \ll N$. The signal x is *compressible* if the representation (1) has just a few large coefficients and many small coefficients.

THE CENTRAL CONCEPT IS STRAIGHTFORWARD: WE TRANSFORM THE IMAGE INTO AN APPROPRIATE BASIS AND THEN CODE ONLY THE IMPORTANT EXPANSION COEFFICIENTS.

$$\mathbf{x} = \sum_{i=1}^{N} s_i \psi_i \quad \text{or} \quad \mathbf{x} = \Psi \mathbf{s} \quad (1)$$

$$\mathbf{y} = \Phi \mathbf{x} = \Phi \Psi \mathbf{s} = \Theta \mathbf{s} \qquad s_i = \langle \mathbf{x}, \psi_i \rangle = \psi_i^T \mathbf{x}$$

Oszczędny pomiar sygnału kompresowalnego:

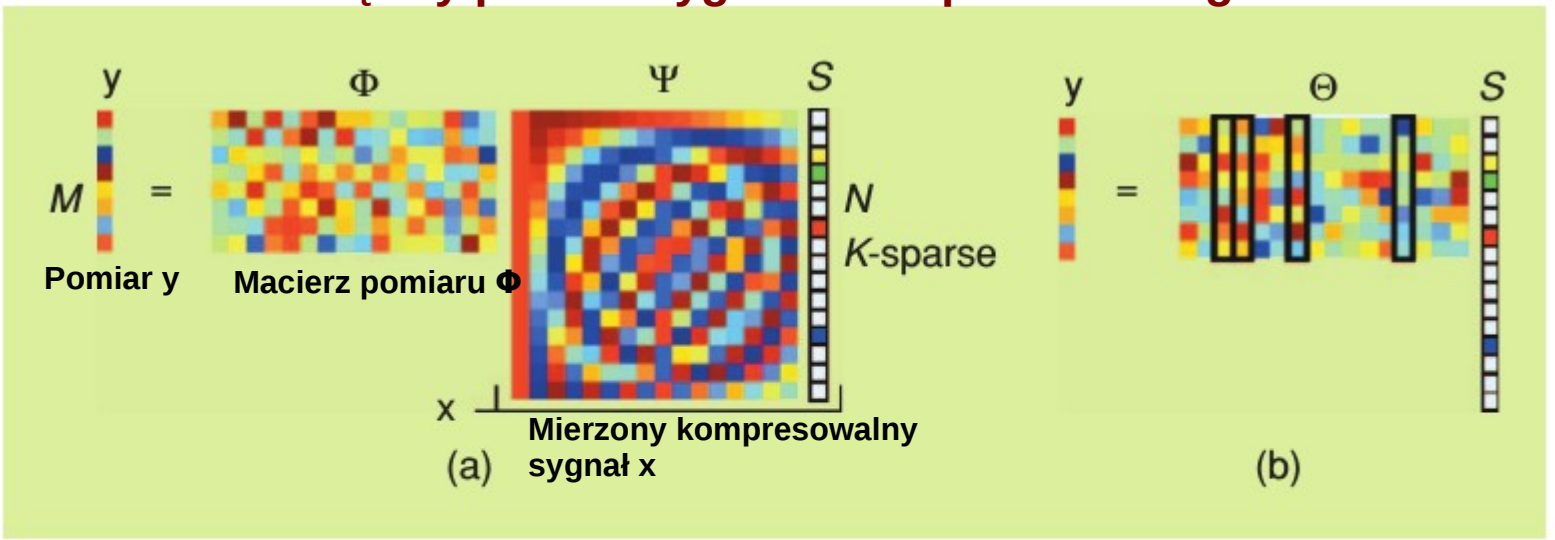

[FIG1] **(a) Compressive sensing measurement process with a random Gaussian measurement matrix Φ and discrete cosine transform (DCT) matrix Ψ. The vector of coefficients s is sparse with $K = 4$. (b) Measurement process with $\Theta = \Phi\Psi$. There are four columns that correspond to nonzero s_i coefficients; the measurement vector y is a linear combination of these columns.**

R. G. Baraniuk, IEEE SIGNAL PROCESSING MAGAZINE, 118, JULY 2007
J. Romberg, IEEE SIGNAL PROCESSING MAGAZINE, 14, MARCH 2008

Idea działania CS - niekoherencja

Jak powinna wyglądać macierz pomiaru Φ , żeby z pomiaru y można było odtworzyć sygnał x ?

CS THEORY ASSERTS THAT ONE CAN RECOVER CERTAIN SIGNALS AND IMAGES FROM FAR FEWER SAMPLES OR MEASUREMENTS THAN TRADITIONAL METHODS USE.

$$\mathbf{y} = \Phi\mathbf{x} = \Phi\Psi\mathbf{s} = \Theta\mathbf{s}$$

(macierz Φ nie jest kwadratowa i w ogólności problem odwrotny nie ma jednoznacznego rozwiązania).

The measurement matrix Φ must allow the reconstruction of the length-N signal $\mathbf{x}$ from $M < N$ measurements (the vector $\mathbf{y}$). Since $M < N$, this problem appears ill-conditioned. If, however, $\mathbf{x}$ is K-sparse and the K locations of the nonzero coefficients in $\mathbf{s}$ are known, then the problem can be solved provided $M \geq K$. A necessary and sufficient condition for this simplified problem to be well conditioned is that, for any vector $\mathbf{v}$ sharing the same K nonzero entries as $\mathbf{s}$ and for some $\epsilon > 0$

$$1 - \epsilon \leq \frac{\|\Theta\mathbf{v}\|_2}{\|\mathbf{v}\|_2} \leq 1 + \epsilon\,. \qquad (3)$$

That is, the matrix Θ must preserve the lengths of these particular K-sparse vectors. Of course, in general the locations of the K nonzero entries in $\mathbf{s}$ are not known. However, a sufficient condition for a stable solution for both K-sparse and compressible signals is that Θ satisfies (3) for an arbitrary $3K$-sparse vector $\mathbf{v}$. This condition is referred to as the *restricted isometry property* (RIP) [1]. A related condition, referred to as *incoherence*, requires that the rows $\{\phi_j\}$ of Φ cannot sparsely represent the columns $\{\psi_i\}$ of Ψ (and vice versa).

R. G. Baraniuk, IEEE SIGNAL PROCESSING MAGAZINE, 118, JULY 2007
J. Romberg, IEEE SIGNAL PROCESSING MAGAZINE, 14, MARCH 2008

Idea działania CS - niekoherencja

Przykład macierzy pomiaru Φ:
- można wybrać zbiór realizacji szumu białego o zerowej średniej i wariancji 1/N

- The matrix Φ is incoherent with the basis $\Psi = \mathbf{I}$ of delta spikes with high probability. More specifically, an $M \times N$ iid Gaussian matrix $\Theta = \Phi\mathbf{I} = \Phi$ can be shown to have the RIP with high probability if $M \geq cK \log(N/K)$, with c a small constant [1], [2], [4]. Therefore, K-sparse and compressible signals of length N can be recovered from only $M \geq cK \log(N/K) \ll N$ random Gaussian measurements.
- The matrix Φ is universal in the sense that $\Theta = \Phi\Psi$ will be iid Gaussian and thus have the RIP with high probability regardless of the choice of orthonormal basis Ψ.

WHAT IS MOST REMARKABLE ABOUT THESE SAMPLING PROTOCOLS IS THAT THEY ALLOW A SENSOR TO VERY EFFICIENTLY CAPTURE THE INFORMATION IN A SPARSE SIGNAL WITHOUT TRYING TO COMPREHEND THAT SIGNAL.

R. G. Baraniuk, IEEE SIGNAL PROCESSING MAGAZINE, 118, JULY 2007
J. Romberg, IEEE SIGNAL PROCESSING MAGAZINE, 14, MARCH 2008

Idea działania CS - rekonstrukcja

Define the ℓ_p norm of the vector s as $(\|\mathbf{s}\|_p)^p = \sum_{i=1}^{N} |s_i|^p$. The classical approach to inverse problems of this type is to find the vector in the translated null space with the smallest ℓ_2

■ **Minimum ℓ_1 norm reconstruction**: Surprisingly, optimization based on the ℓ_1 norm

$$\hat{\mathbf{s}} = \text{argmin} \|\mathbf{s}'\|_1 \text{ such that } \Theta\mathbf{s}' = \mathbf{y}$$

can exactly recover K-sparse signals and closely approximate compressible signals with high probability using only $M \geq cK \log(N/K)$ iid Gaussian measurements [1], [2]. This is a convex optimization problem that conveniently reduces to a linear program known as basis pursuit [1], [2] whose computational complexity is about $O(N^3)$. Other,

Rekonstrukcja poprzez rozwiązanie problemu optymalizacji w sensie normy $\ell 1$ preferuje wektory rzadkie. Jeśli dokładne rozwiązanie jest rzadkie, może zostać znalezione, pomimo iż problem odwrotny nie był dobrze zdefiniowany.

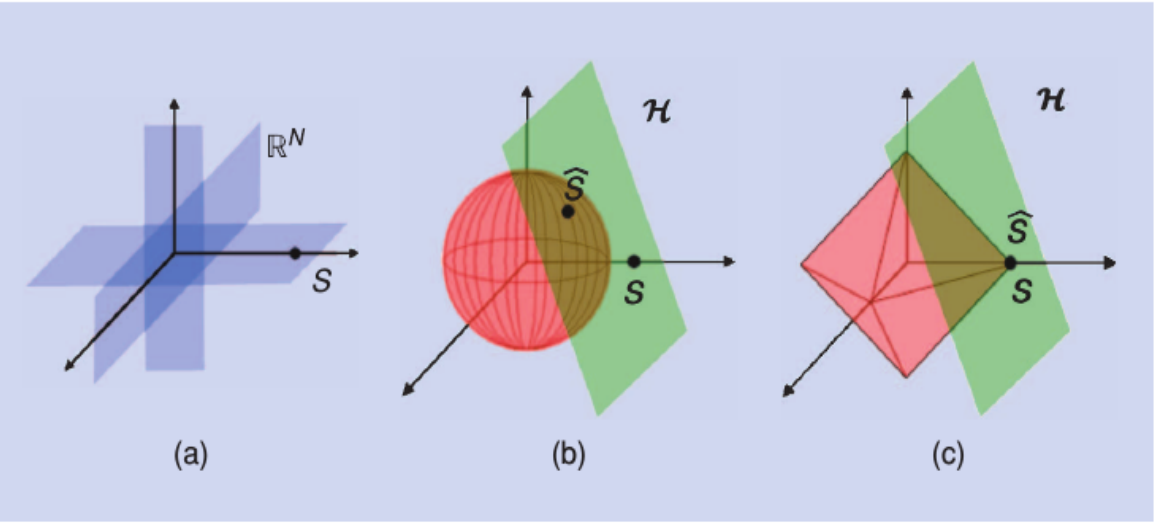

[FIG2] **(a) The subspaces containing two sparse vectors in $\mathbb{R}^3$ lie close to the coordinate axes. (b) Visualization of the ℓ_2 minimization (5) that finds the non-sparse point-of-contact $\hat{s}$ between the ℓ_2 ball (hypersphere, in red) and the translated measurement matrix null space (in green). (c) Visualization of the ℓ_1 minimization solution that finds the sparse point-of-contact $\hat{s}$ with high probability thanks to the pointiness of the ℓ_1 ball.**

R. G. Baraniuk, IEEE SIGNAL PROCESSING MAGAZINE, 118, JULY 2007
J. Romberg, IEEE SIGNAL PROCESSING MAGAZINE, 14, MARCH 2008

http://users.ece.gatech.edu/~justin/l1magic/

ℓ_1-MAGIC

code / papers / links

One of the central tenets of signal processing is the Shannon/Nyquist sampling theory: the number of samples needed to capture a signal is dictated by its bandwidth. Very recently, an alternative theory of "compressive sampling"has emerged. By using nonlinear recovery algorithms (based on convex optimization), super-resolved signals and images can be reconstructed from what appears to be highly incomplete data. Compressive sampling shows us how data compression can be implicitly incorporated into the data acquisition process, a gives us a new vantage point for a diverse set of applications including accelerated tomographic imaging, analog-to-digital conversion, and digital photography.

See examples of compressive sampling in action.

Code

L1-MAGIC is a collection of MATLAB routines for solving the convex optimization programs central to compressive sampling. The algorithms are based on standard interior-point methods, and are suitable for large-scale problems.

Download the code (including User's Guide)
Download the User's Guide (pdf)

L1-magic toolbox

Przykład rozwiązywanego zagadnienia optymalizacji:

- **Min-ℓ_1 with equality constraints.** The program

$$(P_1) \quad \min \ \|x\|_1 \quad \text{subject to} \quad Ax = b,$$

also known as *basis pursuit*, finds the vector with smallest ℓ_1 *norm*

$$\|x\|_1 := \sum_i |x_i|$$

that explains the observations b. As the results in [4, 6] show, if a sufficiently sparse x_0 exists such that $Ax_0 = b$, then (P_1) will find it. When x, A, b have real-valued entries, (P_1) can be recast as an LP (this is discussed in detail in [10]).

Tej postaci jest zagadnienie rekonstrukcji sygnału s:

$$\mathbf{y} = \Phi\mathbf{x} = \Phi\Psi\mathbf{s} = \Theta\mathbf{s}$$

Prace poświęcone CS z różnych dziedzin

http://dsp.rice.edu/cs

- Talks
- Software
- Tutorials and Reviews

Kilka tysięcy (?) artykułów

Multi-Sensor and Distributed Compressive Sensing
Model-based Compressive Sensing
1-Bit Compressive Sensing
Compressive Sensing Recovery Algorithms
Coding and Information Theory
High-Dimensional Geometry
Ell-1 Norm Minimization

Statistical Signal Processing
Machine Learning
Bayesian Methods
Finite Rate of Innovation
Adaptive Sampling Methods for Sparse Recovery
Data Stream Algorithms
Random Sampling
Histogram Maintenance
Dimension Reduction and Embeddings

Applications:
Compressive Imaging
Medical Imaging
Analog-to-Information Conversion
Computational Biology
Geophysical Data Analysis
Hyperspectral Imaging
Compressive Radar
Astronomy
Communications
Surface Metrology
Acoustics, Audio, and Speech Processing
Remote Sensing
Computer Engineering
Computer Graphics
Robotics & Control
Content Based Retrieval
Neuroscience
Optics and Holography
Physics
Fault Identification